J|A|C|S COMMUNICATIONS

Published on Web 02/05/2010

Phthalocyanine Blends Improve Bulk Heterojunction Solar Cells

Alessandro Varotto,[†] Chang-Yong Nam,[‡] Ivana Radivojevic,[†] Joao P. C. Tomé,[§] José A. S. Cavaleiro,[§] Charles T. Black,*[,‡] and Charles Michael Drain*[,†,||]

Department of Chemistry and Biochemistry, Hunter College of The City University of New York, New York, New York 10065, Center for Functional Nanomaterials, Brookhaven National Laboratory, Upton, New York 11973, Department of Chemistry, University of Aveiro, 3810-193 Aveiro, Portugal, and The Rockefeller University, New York, New York 10065

Received September 15, 2009; E-mail: ctblack@bnl.gov; cdrain@hunter.cuny.edu

Low-cost photovoltaic (PV) devices may derive performance benefits from the light-absorbing properties of phthalocyanine organic dyes because of their high extinction coefficients, stability, and energy band gaps well-matched to the incident solar spectrum.[1−4] Despite these desirable attributes, use of phthalocyanines in low-cost solar cells is complicated by their poor solubility in organic solvents (necessitating vacuum deposition processing)[2,5,6] and narrow absorption bandwidths at red (Q-band) and ultraviolet (B-band) wavelengths.[7] Bulk heterojunction (BHJ) solar cells with dyes such as phthalocyanine[5,7,8] and polymer blends have been reported.[9,10] There are several solar cell designs that contain phthalocyanines, especially the zinc and copper complexes, and those that also contain various C_{60} derivatives, wherein the materials are vapor-deposited in specified layers.[11−13] Other soluble dye systems have been incorporated into layered devices or BHJ solar cells.[4,14−16]

We demonstrate a new blend-type parallel tandem solar cell device architecture with several innovative features: (1) Click-type alkylation chemistry on a single commercially available phthalocyanine platform allows the design of a series of robust, chemically compatible dyes with tunable optical band gaps and energy levels. (2) The family of soluble phthalocyanine dyes permits solution-based processing of molecular BHJ solar cells. (3) In these devices, the semiconductor active layer is composed of a blend of three phthalocyanine derivatives having different optical band gaps in order to capture a larger fraction of the solar spectrum. (4) Most significantly, a suitable energy level alignment among the blended dyes creates a parallel tandem connection that increases the current output of the solar cells, since all of the individual dyes contribute to the carrier generation. Furthermore, this scheme is generally applicable to other soluble organic seminconductor blends with proper internal energy alignment.

The ∼70 nm thick blended phthalocyanine active layer provides a disordered tandem device architecture wherein light can be absorbed by materials with successively smaller band gaps and photogenerated charges are collected with a common complementary organic semiconductor. This demonstrates that a hierarchical organization of dyes, wherein the lowest-band-gap (red) dye is at the surface and higher-band-gap (blue) dyes are layered or assembled on top, is not a priori necessary to ensure vectorial charge migration between the electrodes.[2,17] A standard, reproducible, solution-processed device architecture is used to illustrate these points.[9,11]

Scheme 1. Pc Derivatives and the Pyridyl∼C_{60} Derivative (Py∼C_{60}) Used [The Absorption λ_{max} Is Used To Name Each Dye System Because There Are Positional Isomers on the Isoindole; For This Nucleophilic Substitution Reaction, the Outside (β) Positions React First]

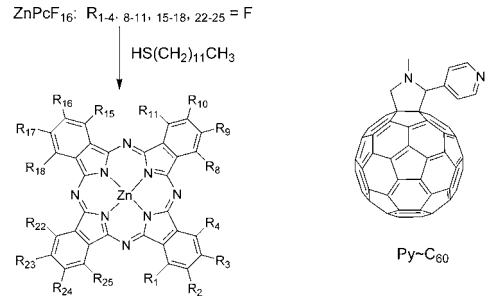

Pc677: R_2 or R_3 + R_9 or R_{10} + R_{16} or R_{17} + R_{23} or R_{24} = *tert*-butyl remaining = H

Pc707: major component has 4 thioalkanes; R_2 or R_3 + R_9 or R_{10} + R_{16} or R_{17} + R_{23} or R_{24} = $S(CH_2)_{11}CH_3$ remaining = F (some with 3 and 5 thioalkanes)

Pc735: major component has 8 thioalkanes; R_2=R_3=R_9=R_{10}=R_{16}=R_{17}=R_{23}=R_{24} = $S(CH_2)_{11}CH_3$ remaining = F (some with 7 and some with 9 thioalkanes)

Pc787: $R_{1\text{-}4,\ 8\text{-}11,\ 15\text{-}18,\ 22\text{-}25}$ = $S(CH_2)_{11}CH_3$

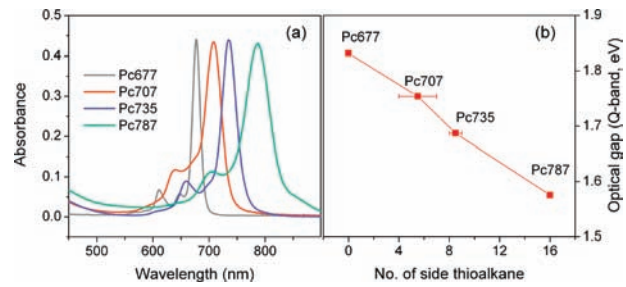

Figure 1. (a) Optical absorbance in toluene normalized to the same absorptivity for the lowest energy Q-band. (b) Q-band HOMO−LUMO gap energy of the Pcs (see the Supporting Information).

We achieve both improved phthalocyanine solubility and control over the optical properties using high-yield substitution of peripheral fluoro groups on hexadecafluorophthalocyaninatozinc(II) ($ZnPcF_{16}$) by thioalkanes [$CH_3(CH_2)_{11}SH$] (Scheme 1).[18,19] Because the frontier molecular orbitals (HOMO and LUMO) are primarily delocalized on the ring periphery, substitution of electron-withdrawing groups with electron-donating groups affects the orbital energy levels.[5,7] The HOMO is destabilized more than the LUMO, resulting in decreased optical band gaps with corresponding maximum absorption wavelengths shifted toward longer wavelengths in the near-IR (Figure 1). Since this effect is additive, one can engineer the light absorption maximum of the dye by balancing the number of electron-donating and -withdrawing substituents (by varying the reaction conditions, including temperature, molar ratio, and base

[†] Hunter College of The City University of New York.
[‡] Brookhaven National Laboratory.
[§] University of Aveiro.
[||] Rockefeller University.

10.1021/ja907851x

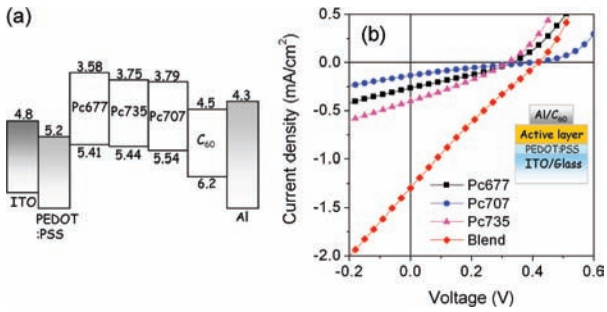

Figure 2. (a) Relative energy levels of the device components (all values in eV). (b) Current−voltage characteristics of solar cells under 1 SUN AM1.5G conditions. The inset shows the cell design.

catalyst; see the Supporting Information). The products are mixtures of isomers and small amounts of the compounds with ±1−2 thioalkanes, so we refer to these products using the wavelength of the Q-band absorption peak in toluene: Pc707, Pc735, and Pc787 (Figure 1). The Pc with four *tert*-butyl groups, ZnPc*t*Bu$_4$ (Pc677) has similar optical absorption spectra and is used because the $ZnPcF_{16}$ starting material has poor solubility. The optical band gaps of the resulting phthalocyanine derivatives (Q-band) decrease nearly linearly from ∼1.83 to 1.58 eV with increasing number of thioalkanes at a rate of ∼16 meV/thioalkane (Figure 1b). We determined the LUMO level of each derivative from the first reduction potentials measured by cyclic voltammetry and the HOMO level by subtracting the Q-band optical band gap from the LUMO level (Figure 2a).

The BHJ solar cells were fabricated with active-layer blends of phthalocyanine derivatives having Py∼C_{60} (see Scheme 1) sandwiched between a poly(3,4-ethylenedioxythiophene):poly-(styrenesulfonate) (PEDOT:PSS) on indium tin oxide (ITO) anode and a C_{60}/Al cathode deposited by thermal evaporation (Figure 2b inset). The C_{60} evaporated on top of the active layer is part of the electrode design and serves to make better contacts between the organic and metallic components. In these devices, the phthalocyanine derivatives provide light absorption and hole transport, while Py∼C_{60}, which can coordinate to the Zn(II) axial positions, facilitates efficient exciton dissociation and electron transport to the electron-collecting contact.[20−22] The spin-cast phthalocyanine active layer consists of either an individual derivative or a blend of Pc677, Pc707, and Pc735. Films formed from Pc787 have an inhomogeneous morphology, and we were unable to form devices from them. For both individual derivatives and blends of dyes, the optimal device active-layer thickness of ∼70 nm was determined by examining device efficiency versus active-layer thickness measured by atomic force microscopy (AFM). The 70 nm thickness represents a balance between maximum incident light absorption and minimal photogenerated carrier recombination. AFM showed that the films have a granular topology with no evidence of domains or phase separation (see the Supporting Information).

The devices were illuminated using a 100 mW/cm^2 simulated solar spectrum (1 SUN AM 1.5G) calibrated using a thermopile detector. Devices having a blend of three Pc derivatives showed significantly improved performance in comparison with devices containing only a single dye (Figure 2b). The blend device short-circuit photocurrent (J_{sc}) of ∼1.24 mA/cm^2 was more than 3 times larger than that of the best single-component device (Pc735, J_{sc} ≈ 0.35 mA/cm^2) and larger than the combined photocurrent from the three individual dye devices (Figure 2b and Table 1), suggesting that a blended Pc architecture significantly improves the efficiency of photoconversion beyond just the increased light absorption. Tandem organic photovoltaic cells, wherein different thermally evaporated dyes reside in different stacked devices (multijunction cells), can have more than twice the photoconversion efficiency of designs with a single dye.[11,23] For the devices reported herein, the best-performing one found to date has a Pc677/Pc707/Pc735 chromophore ratio of 17:17:66 (w/w) with 30% Py∼C_{60} relative to the total amounts of dye. Devices having single derivatives in the active layer (Pc677, Pc707, or Pc735) delivered J_{sc} = 0.14−0.35 mA/cm^2 (Table 1), similar to recent, previously reported values for this type of cell.[17] Additional smaller increases in the open-circuit voltage (V_{oc}) of the dye-blend device, combined with the enhanced J_{sc}, improve the overall power conversion efficiency by a factor of 4, from 0.01−0.03% for individual derivatives to 0.12% for the dye-blended device.

Table 1. Mean PV Parameters of Devices Illuminated with Simulated 1 SUN AM1.5G[a]

	Pc677	Pc707	Pc735	blend
η (%)	0.026	0.012	0.033	0.12
J_{SC} (mA/cm^2)	0.26	0.14	0.35	1.24
V_{OC} (V)	0.351	0.375	0.305	0.408
FF	0.29	0.23	0.3	0.24

[a] The power conversion efficiency (η) of solar cells is given by the expression $\eta = J_{sc} \cdot V_{oc} \cdot \mathrm{FF}$, where J_{sc} is the short-circuit current, V_{oc} is the open-circuit voltage, and FF is the fill factor.

The primary performance benefit of the blend device is an increased J_{sc} due to the three Pc derivative blend components contributing to absorption at different photon energies. Improper relative alignment of the energy levels of the Pc derivatives as well as C_{60} could prevent this device architecture from operating because the individual derivatives may act as carrier recombination centers. An energy diagram constructed from cyclic voltammetry and optical absorption data (Figure 2a) shows possible "staircase energy alignments" for both the HOMO and LUMO levels within the blend, suggesting that regardless of their spatial position in the blend layer, generated free holes and electrons always have pathways to the collecting electrodes without recombination in energetically isolated regions. Direct evidence of the contribution of each Pc derivative to free-carrier generation was obtained by comparing the blend active-layer absorbance to the device input photon-to-current conversion efficiency (IPCE). The blend film shows a broad absorbance peak at 600−800 nm resulting from the sum of the optical spectra of the individual Pc derivatives dominated by the Q-bands, and the IPCE response has a nearly identical spectral shape, indicating that each type of derivative contributes to both light absorption and charge generation (Figure 3). Thus, an estimate of the device internal quantum efficiency of ∼2.5%/0.1 ≈ 25% across all absorbing wavelengths suggests that exciton dissociation and charge collection are equally efficient for all of the Pc blend components.

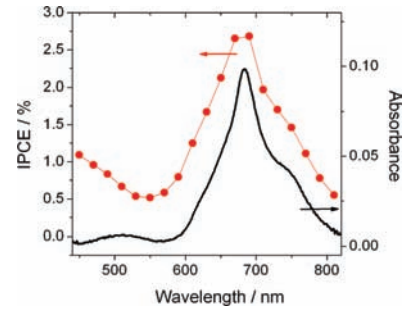

Figure 3. Comparison of the IPCE and the absorbance of the blend device.

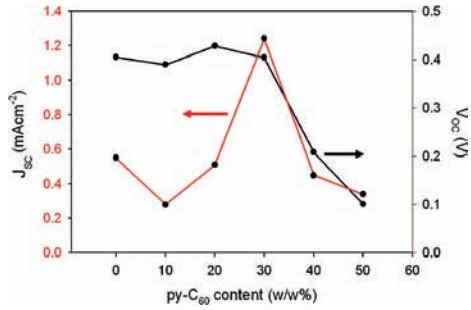

Figure 4. Variation of V_{oc} and J_{sc} vs Py∼C_{60} content in the blend [17:17:66 (w/w) Pc677/Pc707/Pc735].

The best-performing Pc blend device built without mixing Py∼C_{60} into the active layer displayed approximately half of the efficiency, likely because of less efficient charge separation.[24] The Py∼C_{60} derivative is a good electron acceptor with fast kinetics,[25,26] and thus, Py∼C_{60} coordination is a key part of the active-layer design, as also indicated by the poor performance of cells with active layers blended with underivatized C_{60}. ZnPc generally binds one axial pyridine to form five-coordinate complexes. In the present case, the best devices have an approximately 2:1 ZnPc dye/Py∼C_{60} molar ratio (Figure 4). These observations may indicate charge transfer from a noncoordinated ZnPc to a fullerene on a neighboring dye, thereby creating a greater charge separation and contributing to the device performance.[27]

In summary, we have demonstrated the new concept of a blended active layer forming a parallel tandem device architecture using bulk heterojunction solar cells made of self-organized blends of Pc derivatives with engineered optical band gaps and energy levels. $CuPcF_{16}$ is amenable to same fluorine substitution reactions. In combination with an internal parallel connection, the increased solar spectrum coverage of the blend widens the energy range for converting photons into free carriers, resulting in a ∼4-fold increase in J_{sc} and PV conversion efficiency relative to any given Pc component. The suitable alignment of HOMO and LUMO levels among the Pc derivatives and a common complementary fullerene acceptor are key for enabling parallel charge-carrier collection from the device. This new organic PV device scheme is in principle applicable to other blend systems made of high-performance small molecules and conjugated polymers[28−30] with proper energy alignment and may enable higher PV conversion efficiencies, thereby facilitating development of practical organic solar cells.

Acknowledgment. This work was supported by the National Science Foundation (NSF, CHE-0847997 to C.M.D.), and a Goldhaber Distinguished Fellowship to C.-Y.N. Hunter College science infrastructure is supported by the NSF, the National Institutes of Health (including RCMI, G12-RR-03037), and CUNY. Research was carried out in part at the Center for Functional Nanomaterials, Brookhaven National Laboratory, which is supported by the U.S. Department of Energy, Office of Basic Energy Sciences, under Contract No. DE-AC02-98CH10886. We thank Mr. Matthew Jurow for assistance with some of the control experiments and for duplicating the results described herein.

Supporting Information Available: Pc syntheses and device preparation and characterization. This material is available free of charge via the Internet at http://pubs.acs.org.

References

(1) *Phthalocyanines: Properties and Applications*; Leznoff, C. C., Lever, A. B. P., Eds.; Wiley-VCH: New York, 1993; Vols. *2* and 3.
(2) Peumans, P.; Yakimov, A.; Forrest, S. R. *J. Appl. Phys.* **2003**, *93*, 3693.
(3) Xue, J.; Rand, B. P.; Uchida, S.; Forrest, S. R. *Adv. Mater.* **2005**, *17*, 66.
(4) Perez, M. D.; Borek, C.; Forrest, S. R.; Thompson, M. E. *J. Am. Chem. Soc.* **2009**, *131*, 9281.
(5) de la Torre, G.; Claessens, C. G.; Torres, T. *Chem. Commun.* **2007**, 2000.
(6) Rand, B. P.; Genoe, J.; Heremans, P.; Poortmans, J. *Prog. Photovoltaics* **2007**, *15*, 659.
(7) Rio, Y.; Rodrıguez-Morgade, M. S.; Torres, T. *Org. Biomol. Chem.* **2008**, *6*, 1877.
(8) Honda, S.; Nogami, T.; Ohkita, H.; Benten, H.; Ito, S. *Appl. Mater. Interfaces* **2009**, *1*, 804.
(9) Kim, J. Y.; Qin, Y.; Stevens, D. M.; Ugurlu, O.; Kalihari, V.; Hillmyer, M. A.; Frisbie, C. D. *J. Phys. Chem. C* **2009**, *113*, 10790.
(10) Rajaram, S.; Armstrong, P. B.; Kim, B. J.; Fréchet, J. M. J. *Chem. Mater.* **2009**, *21*, 1775.
(11) Ameri, T.; Dennler, G.; Lungenschmied, C.; Brabec, C. J. *Energy Environ. Sci.* **2009**, *2*, 347.
(12) Chu, W. P.; Tsai, Y. S.; Juang, F. S.; Li, T. S.; Chung, C. H. *PIERS Online* **2007**, *3*, 825.
(13) Koeppe, R.; Sariciftci, N. S.; Troshin, P. A.; Lyubovskaya, R. N. *Appl. Phys. Lett.* **2005**, *87*, 244102.
(14) Walker, B.; Tamayo, A. B.; Dang, X.-D.; Zalar, P.; Seo, J. H.; Garcia, A.; Tantiwiwat, M.; Nguyen, T.-Q. *Adv. Funct. Mater.* **2009**, *19*, 3063.
(15) Hamann, T. W.; Jensen, R. A.; Martinson, A. B. F.; Ryswyk, H. V.; Hupp, J. T. *Energy Eviron. Sci.* **2008**, *1*, 66.
(16) Kim, J. Y.; Lee, K.; Coates, N. E.; Moses, D.; Nguyen, T.-Q.; Dante, M.; Heeger, A. J. *Science* **2007**, *317*, 222.
(17) Loi, M. A.; Denk, P.; Hoppe, H.; Neugebauer, H.; Winder, C.; Meissner, D.; Brabec, C.; Sariciftci, N. S.; Gouloumis, A.; Vázquez, P.; Torres, T. *J. Mater. Chem.* **2003**, *13*, 700.
(18) Leznoff, C.; Sosa-Sanchez, J. L. Patent WO 2005/033110 A1, 2005.
(19) Leznoff, C. C.; Sosa-Sanchez, J. L. *Chem. Commun.* **2004**, 338.
(20) Drain, C. M.; Varotto, A.; Radivojevic, I. *Chem. Rev.* **2009**, *109*, 1630.
(21) D'Souza, F.; Ito, O. *Coord. Chem. Rev.* **2005**, *249*, 1410.
(22) Troshin, P. A.; Koeppe, R.; Peregudov, A. S.; Peregudova, S. M.; Egginger, M.; Lyubovskaya, R. N.; Sariciftci, N. S. *Chem. Mater.* **2007**, *19*, 5363.
(23) Yakimov, A.; Forrest, S. R. *Appl. Phys. Lett.* **2002**, *80*, 1667.
(24) Brütting, W.; Bronner, M.; Götzenbrugger, M.; Opitz, A. *Macromol. Symp.* **2008**, *268*, 38.
(25) Illescas, B. M.; Martín, N. C. R. *Chimie* **2006**, *9*, 1038.
(26) Guldi, D. M.; Prato, M. *Acc. Chem. Res.* **2000**, *33*, 695.
(27) Honda, S.; Nogami, T.; Ohkita, H.; Benten, H.; Ito, S. *ACS Appl. Mater. Interfaces* **2009**, *1*, 804.
(28) Egginger, M.; Koeppe, R.; Meghdadi, F.; Troshin, P. A.; Lyubovskaya, R. N.; Meissner, D.; Sariciftci, N. S. *Proc. SPIE* **2006**, *6192*, 61921Y.
(29) Mak, C. S. K.; Leung, Q. Y.; Chan, W. K.; Djurišić, A. B. *Nanotechnology* **2008**, *19*, 424008.
(30) Martínez-Díaz, M. V.; Díaz, D. D. *J. Porphyrins Phthalocyanines* **2009**, *13*, 397.

JA907851X